Polarization coded aperture

Wanli Chi, Kaiqin Chu and Nicholas George

The Institute of Optics, University of Rochester, Rochester NY 14627

chiw@optics.rochester.edu

Abstract: Two examples are presented to illustrate the advantages of polarization coded apertures, in which the incoming light will rotate its polarization at a portion of an aperture. In the first example the depth of field of a diffraction limited lens is increased without sacrificing the light throughput; in the second example the axial focal intensity of a pixelated Fresnel zone plate is increased by 100%. Both examples work for linearly polarized or unpolarized illumination.

OCIS codes: (110.1220) apertures; (260.5430) polarization; (999.9999) depth of field; (999.9999) Fresnel zone plate.

References and links

1. A. Ghosh, K. Murata and A. K. Chakraborty, "Frequency-response characteristics of a perfect lens masked by polarizing devices," J. Opt. Soc. Am. A **5,** 277–284 (1988).
2. D. R. Chowdhury, K. Bhattacharya, S. Sanyal and A. K. Chakraborty, "Performance of a polarization-masked lens aperture in the presence of spherical aberration," J. Opt. A: Pure and Applied Optics, **4,** 98–104 (2002).
3. A. Zlotnik, Z. Zalevsky and E. Marom, "Superresolution with nonorthogonal polarization coding," Appl. Opt. **44,** 3705–3715 (2005).
4. E. H. Linfoot and E. Wolf, "Diffraction images in systems with an annular aperture," Proc. Phys. Soc. B **66,** 145–149 (1953).
5. T-C Poon and M. Motamedi, "Optical digital incoherent image-processing for extended depth of field," Appl. Opt. **26,** 4612–4615 (1987).
6. J. Ojeda-Castaneda and L. R. Berriel Valdos, "Abitrarily high focal depth with finite aperture," Opt. Lett. **13,** 183–185 (1988).
7. E. R. Dowski, Jr. and W. T. Cathey, "Extended depth of field through wave-front coding," Appl. Opt. **34,** 1859–1866 (1995).
8. W. Chi and N. George, "Computational imaging with the logarithmic asphere: theory," J. Opt. Soc. Am. A **20,** 2260–2273 (2003).
9. P. Yeh and C. Gu, *Optics of Liquid Crystal Displays,* (John Wiley & Sons, Inc., New York, 1999). Chapter 9 and references therein.
10. T. D. Beynon, I. Kirk and T. R. Mathews, "Gabor zone plate with binary transmittance values," Opt. Lett. **17,** 544–546 (1992).
11. P. W. McOwan, M. S. Gordon and W. J. Hossack, "A switchable liquid crystal binary Gabor lens," Opt. Commun. **103,** 189–193 (1993).
12. R. E. English, Jr. and N. George, "Diffraction from a circular aperture: on axis field strength," Appl. Opt. **26,** 2360-2363 (1987).

1. Introduction

New imaging devices or better imaging properties can be obtained by utilizing the polarization of an electromagnetic (EM) wave [1]-[3]. In this paper we describe a novel polarization coding technique applied to the aperture of an imaging system. As the light passes through the aperture, the polarization of the incoming beam is rotated for a portion of the aperture while it is not rotated for the remaining portion. At the image plane the detector senses the two independent

#71216 - $15.00 USD Received 22 May 2006; revised 20 June 2006; accepted 20 June 2006

orthogonal intensities of the polarized light. This polarization coded aperture system results in better imaging systems. In the first example, we show that the depth of field of a diffraction limited lens is improved. In the second example, we explain a pixelated Fresnel zone plate whose efficiency is doubled over that for conventional zone plate. Practical system implementation is made possible with current liquid crystal technology. This polarization coded aperture technique does not put any strict constraint on the polarization of illumination, since it works for either linear polarized or unpolarized illumination.

2. Extended depth of field

It is well known that the depth of field of a diffraction limited lens depends on its numerical aperture. The depth of field of a diffraction limited lens with clear aperture is proportional to the square of f-number. So for a diffraction limited lens with focal length f and clear circular aperture whose radius is R, the depth of field is inversely proportional to the area of the aperture. (The same statement is also held for ring aperture [4, 5], i.e., the depth of field for a ring aperture with radius from r to R is also inversely proportional to the area of the ring aperture.) Achieving the extended depth of field by reducing the aperture size is routinely done in photography. Also in the literature one uses various apodizations [4]-[6] e.g., a central obscuration, to extend the depth of field. The main disadvantage of the apodization method is that it decreases the light throughput and thus is not a good solution in low light level imaging applications. In this section, we introduce a type of polarization coding in the aperture of a diffraction limited lens to extend the depth of field. Consider a diffraction limited lens with a circular aperture shown in Fig. 1. The aperture with a radius of R is separated into two regions of equal area, the central circular region with a radius of r and the outer circular ring region with $R = \sqrt{2}r$. The polarization of the EM wave passing the outer ring region will be kept the same, and the polarization of the EM wave passing the central region will be rotated by 90^0. With the advancement in liquid crystal technology, there is no difficulty in realizing this type of aperture. Here we consider only the case with incoherent illumination.

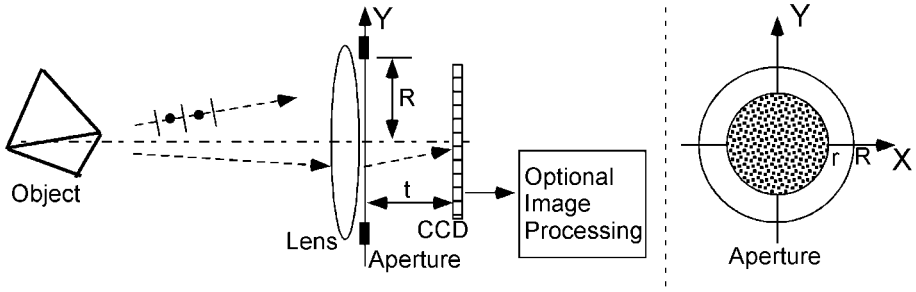

Fig. 1. The extended depth of field imaging setup with a polarization coded aperture.

When the incoming EM wave is polarized in Y direction, after passing the outer region of the aperture, the wave is still polarized in Y direction; but after passing the inner region of the aperture, the wave changes its polarization to the X direction. Since the CCD detects intensity proportional to $\mathbf{E} \cdot \mathbf{E}^*$, there is no interference between EM waves in orthogonal direction. The intensity point spread function (IPSF) of this imaging setup is obtained by the addition of two IPSFs of a diffraction limited lens, one with a circular aperture and another with a ring aperture shown shaded. This statement also holds for two other important cases: one where the EM wave is X-polarized and the other when the incoming light is unpolarized. Hence, in general one can write the intensity point spread function $I(\rho)$ for the Fig. 1 system as follows:

#71216 - $15.00 USD Received 22 May 2006; revised 20 June 2006; accepted 20 June 2006

$$I(\rho)=\left|\int_0^r r' J_0(2\pi r'\frac{\rho}{\lambda t})\exp[i\frac{2\pi W}{\lambda}(\frac{r'}{R})^2]dr'\right|^2+\left|\int_r^R r' J_0(2\pi r'\frac{\rho}{\lambda t})\exp[i\frac{2\pi W}{\lambda}(\frac{r'}{R})^2]dr'\right|^2, \quad (1)$$

where a constant is dropped, ρ is the radial coordinate of the IPSF, λ is the wavelength of illumination, W is the defocus coefficient in the unit of number of wavelengths, and J_0 denotes the Bessel function of first type order zero. Since the principle works well for unpolarized light, no polarizer is needed to filter the incoming light.

The first term in Eq. (1) is the point spread function for central clear aperture with a radius of r; the second term is the point spread function for a ring aperture with radius from r to R. It is interesting to note that the constant phase delay introduced by the liquid crystal located at the central region of the aperture has no effect on the IPSF of the system. In Fig. 2 we show these intensity point spread functions. When $W=0$, It is observed that the IPSF for the ring aperture has a narrower central peak than that for full aperture and that the IPSF of the central aperture has a wider central peak. At the focused position the IPSF for the polarization coded aperture is the sum of IPSFs of central and ring apertures. In Fig. 2, we also plotted the IPSFs for a full aperture with defocus coefficient $W=0.5\lambda$. The axial intensity of this IPSF is about 40% of that for full aperture without defocus.

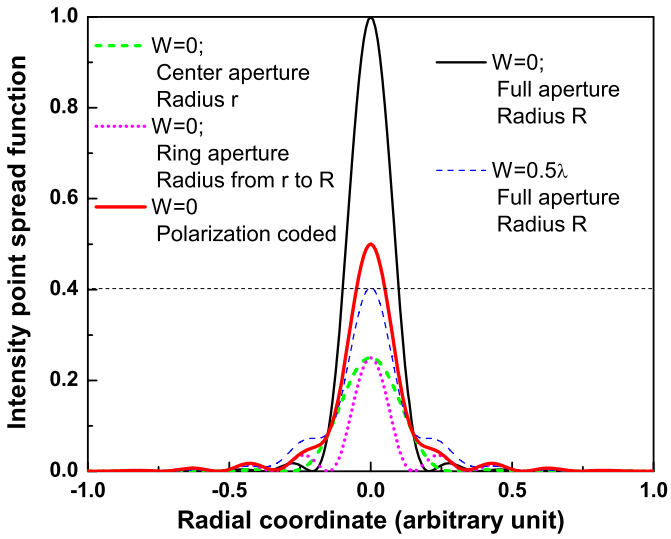

Fig. 2. The IPSFs of diffraction limited lens for central aperture; ring aperture and full aperture.

Since the depth of field is inversely proportional to the area of the aperture, so by separating the aperture into central clear aperture and outer ring aperture region with equal areas. We expected the depth of field is increased by a factor of 2 for central region and outer region respectively. Since the IPSFs of the two aperture regions are detected without amplitude interference, as explicit in Eq. (1), the depth of field of the polarization coded aperture system in Fig. 1 is also increased by a factor of 2. To qualitatively illustrate the increase in the depth of field, we show in Figs. 3 and 4 the IPSFs for a lens with polarization coded aperture and a lens

#71216 - $15.00 USD Received 22 May 2006; revised 20 June 2006; accepted 20 June 2006

with conventional aperture, respectively. The defocus amounts in these two figures are set to be from $W = 0.5\lambda$ to 1.25λ. The intensities are normalized such that the axial intensity of the IPSF at the focused position for a full clear aperture with radius R is 1 (see Fig. 2). By comparing the size of IPSFs in Figs. 3 and 4 as the offset distance in location of object, as measured by defocus W, we see the substantial increase in the depth of field. Figures 5 and 6 show the Optical Transfer Functions (OTFs) corresponding to Figs. 3 and 4, respectively. We observe contrast inversions for a conventional aperture when defocus is 0.75λ, λ and 1.25λ; but there are no such contrast inversion for the polarization coded aperture and the OTFs are positive for all the spatial frequencies. This increase in depth of field can be easily understood since both cutdown the aperture (central region) and central aperture obscuration (outer region) induce the increase in depth of field.

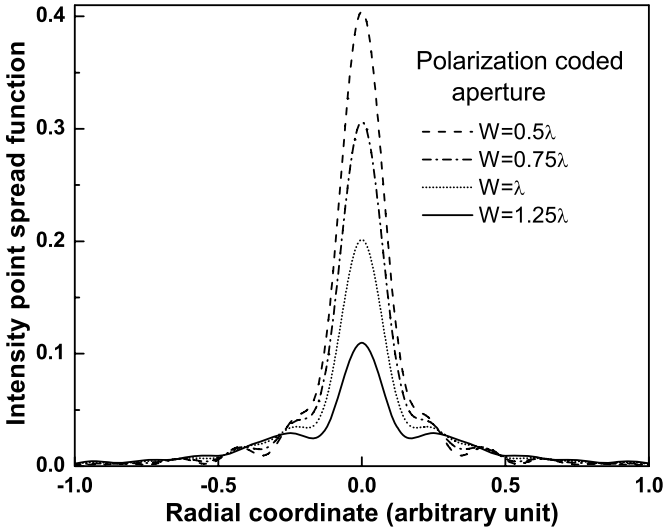

Fig. 3. The IPSFs of diffraction limited lens for a lens with polarization coded aperture.

When the incoming beam, e.g., from the off-axis object point, is obliquely incident to the central region of aperture, shown in Fig. 1, where the liquid crystal is present for polarization rotation, the rotation angle will be deviated from 90^0. This will affect the depth of field extension for large field of view. For a conventional liquid crystal aperture, a half field of view of 15^0 is anticipated. However, various techniques [9] have been developed to improve the wide angle performance of the liquid crystal devices, which extend the half angle performance to well over 50^0.

We expect this type of polarization coded aperture for extended depth of field to be extremely useful for low ambient light illumination since the optical throughput is the same as that for a big clear aperture with radius R. Another interesting feature of this design is that no aberration is introduced to the diffraction limited lens, so it is not necessary to deblur the detector image using digital processing techniques, which generally is required for the cubic phase mask method [7] and the logarithmic asphere method [8]. However, one still can choose to use the image processing to boost the high spatial frequency response, this is optional.

#71216 - $15.00 USD Received 22 May 2006; revised 20 June 2006; accepted 20 June 2006

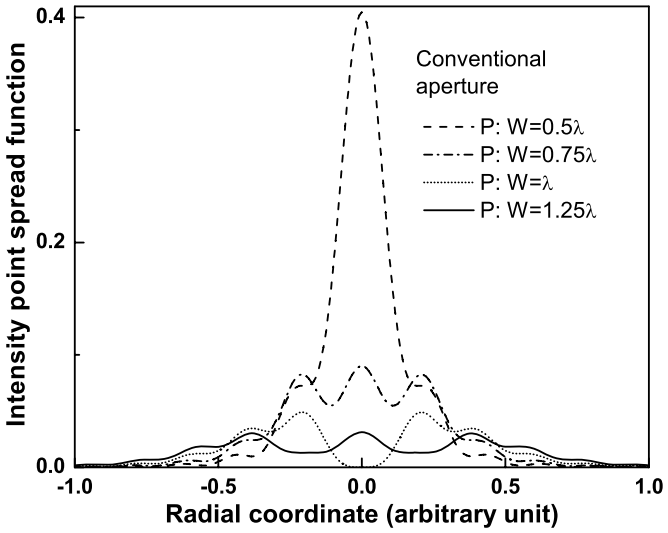

Fig. 4. The IPSFs of diffraction limited lens for a lens with conventional aperture.

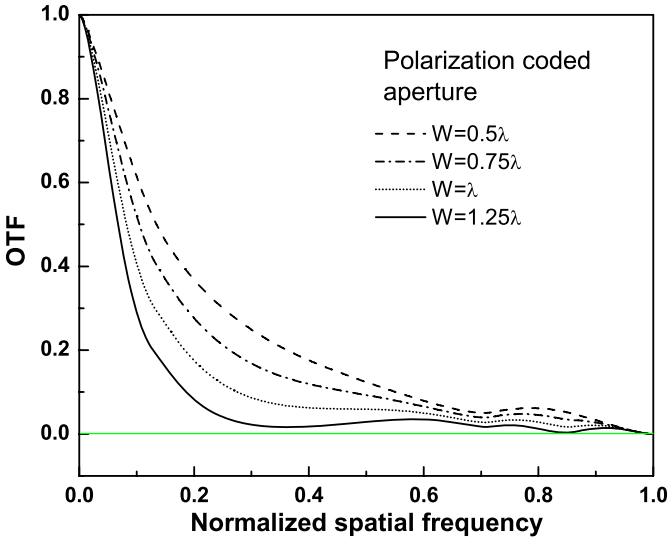

Fig. 5. The OTFs of diffraction limited lens for a lens with polarization coded aperture.

#71216 - $15.00 USD Received 22 May 2006; revised 20 June 2006; accepted 20 June 2006

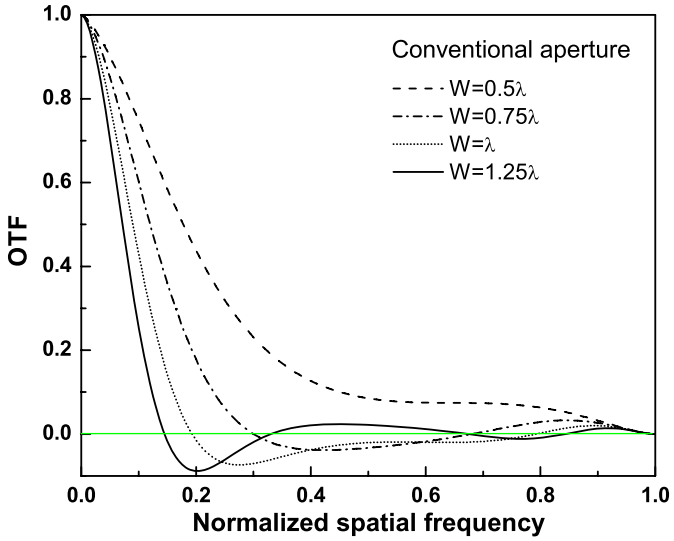

Fig. 6. The OTFs of diffraction limited lens for a lens with conventional circular aperture.

3. Pixelated Fresnel zone plate

Binary zone plates are diffractive elements with a binary transmission function. Common examples include the Fresnel zone plate, Beynon zone plate or binary Gabor zone plate [10, 11]. Generally, the total transmission of the binary zone plate is around 50%. i.e., half of incoming light energy is absorbed by the zone plate. Using the polarization coding idea, we impose a 90^0 polarization rotation for the zero transmission pixels of a zone plate. In this way the zone plate is effectively separated into two plates with orthogonal output polarizations. This yields an increase in the efficiency of the binary zone plate by 100%. In this section a pixelated Fresnel zone plate with a polarization coded aperture using a liquid crystal spatial light modulator (SLM) is described.

Consider the setup shown in Fig. 7. A plane wave is modulated by the SLM zone plate, which has a pixel size of a. The modulation takes two forms, the polarization of light is either rotated by 90^0 or not rotated by each pixel. After passing the SLM, the light is focused to point P, which is located at a distance f from the zone plate. The zone plate shown in Fig. 7 is called a pixelated zone plate since the smallest structure of the zone plate is the pixel size of the liquid crystal device.

To determine the optimum state of each pixel, we calculate the field contribution of each pixel to the axial point P. The axis field amplitude at focal point P, E_{mn}, from the contribution of pixel (x_m, y_n) is

$$E_{mn} = A \int_{y_n - a/2}^{y_n + a/2} \int_{x_m - a/2}^{x_m - a/2} \frac{f}{f^2 + x^2 + y^2} \exp(i \frac{2\pi}{\lambda} \sqrt{f^2 + x^2 + y^2}) dx dy, \qquad (2)$$

where A is a constant, λ is the wavelength of incoming plane wave. After evaluating this integral numerically, we can write the result in a form of $E_{mn} = |E_{mn}| \exp[i\phi_{mn}]$. Herein, We consider only the binary type plate. i.e., the polarization either changed by 90^0 or not changed and no amplitude or phase modulation is introduced. If the phase term ϕ_{mn} satisfies $-\pi/2 \leq \phi_{mn} < \pi/2$,

#71216 - $15.00 USD Received 22 May 2006; revised 20 June 2006; accepted 20 June 2006

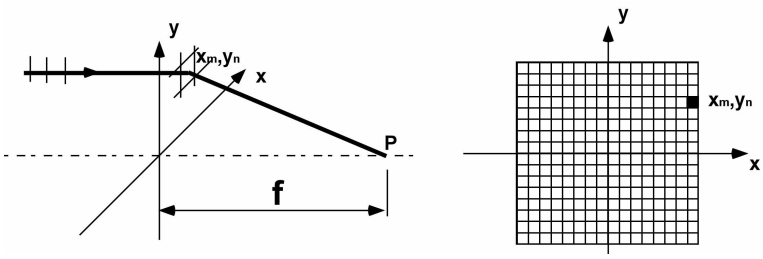

Fig. 7. The setup for pixelated zone plate. Left: setup; Right: pixelated zone plate

then we set the pixel (m,n) to be transmissive without rotation of polarization. Otherwise, if $-\pi \le \phi_{mn} < -\pi/2$ or $\pi/2 \le \phi < \pi$, we set the pixel be transmissive with a 90^0 rotation of the incoming wave polarization. Because EM waves with orthogonal polarizations do not interfere, the axial intensity at the focal point P can be written as following:

$$I_P = \left| \sum_{-\pi/2 \le \phi_{mn} < \pi/2} E_{mn} \right|^2 + \left| \sum_{-\pi \le \phi_{mn} < -\pi/2 \text{ or } \pi/2 \le \phi_{mn} < \pi} E_{mn} \right|^2 . \tag{3}$$

In Eq. (3) the first term is the axial intensity for a zone plate without polarization coding, and the second term is the axial intensity for another zone plate in which the pass and block pixels are complementary to the first plate. Theses two plates have approximately equal axial focal intensity independent of the fill factor of zone plates. Both terms in Eq. (3) change in the same manner if the fill factor of the zone zone plate is changed. so we have

$$I_P \simeq 2 \left| \sum_{-\pi/2 \le \phi_{mn} < \pi/2} E_{mn} \right|^2 . \tag{4}$$

i.e., the axial intensity of polarization coded binary zone plate is increased by 100% compared to the binary zone plate with 0 and 1 transmissions. This conclusion is valid independent of the liquid crystal zone plate fill factor.

Figure 8 shows one example of the pixelated Fresnel zone plate. In this example $f = 100mm$, $a = 15\mu m$ and $\lambda = 0.6\mu m$. The white pixel denotes that the EM field will keep its polarization after passing the plate and black pixel denotes that the EM field will rotate 90^0 after passing the plate. We note that the center region of the pixelated zone plate resembles a Fresnel zone plate. Due to the finite size of pixel sampling, the outer region deviates from the Fresnel zone plate. We call this plate the pixelated Fresnel zone plate with polarization coded aperture. Similar to the system described in Fig. 1, this pixelated Fresnel zone plate works for both linearly polarized and unpolarized light.

Figure 9 shows the computer simulation result of the axial intensities of the pixelated zone plates. The results of plates both with and without polarization coded aperture are shown. The polarization coded plate used in this simulation is shown in Fig. 8; and with the reference of Fig. 8, The pixelated zone plate without polarization coding has a transmission of 1 for white pixels and 0 for black pixels. It is clear in Fig. 9 that the axial intensity is increased by 100% for the polarization coded plate. Higher order focal points can be seen at positions of $f/3$, $f/5$, etc. Besides the doubling of the axial intensity for focal point P due to polarization coding of the zone plate aperture, an interesting effect of finite pixel size of SLM is that the axial intensity of higher order focal points is significantly lower than that of 1st order. (This is in contrast with the conventional Fresnel zone plate where the axial intensities of different order focal points

#71216 - $15.00 USD Received 22 May 2006; revised 20 June 2006; accepted 20 June 2006

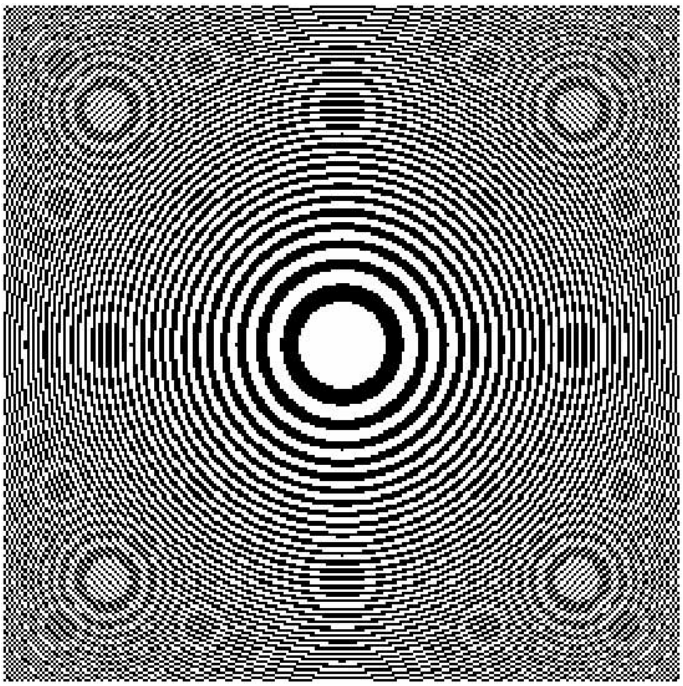

Fig. 8. A pixelated Fresnel zone plate. White pixel: no change in polarization; black pixel: polarization rotate 90^0.

are equal.) From Eq. (2), one can also calculate the polarization status of different orders. For example, if the input beam is linearly polarized, then the polarizations of the 1st order and zeroth order beam are orthogonal.

4. Conclusion

The polarization state at the aperture of an imaging system can be modified to yield a better imaging properties. Specifically in this paper, we describe a novel configuration where the polarization is rotated by 90^0 at a portion of aperture and kept the same for the rest of aperture. Since there is no interference between polarizations in orthogonal directions, this coded aperture is equivalent to the adding of two apertures. Since the principle works for both linear polarized and unpolarized light, no polarizer is required to filter the illumination light and there is no compromise of the light throughput. Using this polarized coded aperture concept, in the first example we show the extended depth of field imaging of a diffraction limited lens (by a factor of 2 without image processing) is achieved without sacrificing detector light intensity and is good for low light level imaging. The extended depth of field The optional image processing can also be done easily since there are no zero's and negatives in the OTF over a significant amount of defocus, as seen in Fig. 5. In the second example a pixelated Fresnel zone plate with polarization coding is illustrated which yields a 100% increase in diffraction efficiency. This research was supported in part by the Army Research Office.

5. Appendix:Axial intensity of Fresnel zone plate

Consider a Fresnel zone plate which has a focal length of f and $2N-1$ zones with the center first zone transmissive. The transmission function can be written as

#71216 - $15.00 USD Received 22 May 2006; revised 20 June 2006; accepted 20 June 2006

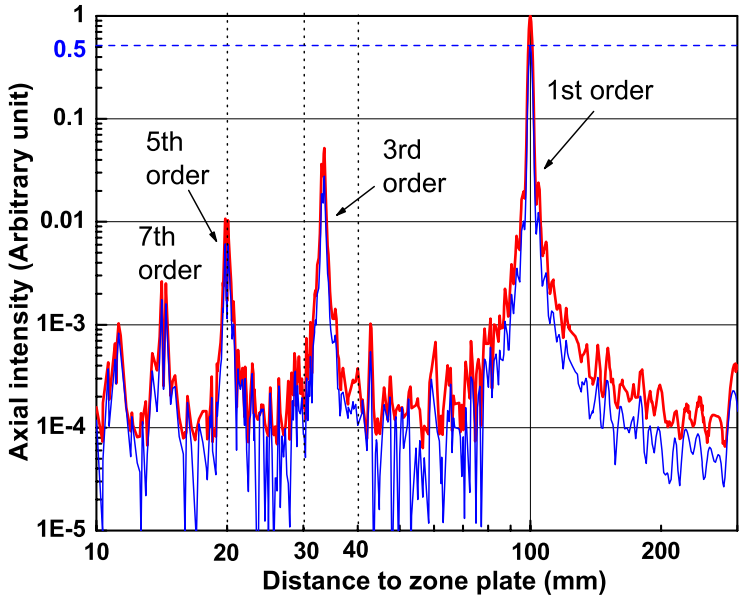

Fig. 9. Axial intensity of pixelated zone plates with and without polarization coded aperture. Thick red line: pixelated zone plate with polarization coded aperture as shown in Fig. 8; Thin blue line: pixelated zone plate without polarization coding.

$$t(r) = \sum_{n=1}^{2N-1} (-1)^{n+1} \mathrm{circ}(r/r_n), \tag{5}$$

where r is the radial coordinate of the zone plate and $r_n = \sqrt{n\lambda f}$.

For plane wave illumination with amplitude E_0, the axial field amplitude $E(z)$ at a distance of z can be written as

$$E(z) = \sum_{n=1}^{2N-1} (-1)^{n+1} E(z,n), \tag{6}$$

where $E(z,n)$ is the amplitude contribution for a circular aperture with radius r_n. $E(z,n)$ of Eq. (6) can be evaluated [12] exactly with the following result:

$$E(z,n) = E_0[\exp(i\frac{2\pi}{\lambda}z) - \frac{z}{\sqrt{z^2+r_n^2}}\exp(i\frac{2\pi}{\lambda}\sqrt{z^2+r_n^2})]. \tag{7}$$

Substitution of Eq. (7) into Eq. (6) and squaring gives the axial intensity of the zone plate at a distance z as follows:

$$I(z) = C\left|e^{i\frac{2\pi}{\lambda}z} + \sum_{n=1}^{2N-1} (-1)^n \frac{z}{\sqrt{z^2+n\lambda f}}\exp(i\frac{2\pi}{\lambda}\sqrt{z^2+n\lambda f})\right|^2, \tag{8}$$

where C is a constant.

#71216 - $15.00 USD
Received 22 May 2006; revised 20 June 2006; accepted 20 June 2006